Role of Ubiquitin C-Terminal Hydrolase-L1 in Antipolyspermy Defense of Mammalian Oocytes 1

Authors: Susor, Andrej, Liskova, Lucie, Toralova, Tereza, Pavlok, Antonin, Pivonkova, Katerina, et al.

Source: Biology of Reproduction, 82(6) : 1151-1161

Published By: Society for the Study of Reproduction

URL: https://doi.org/10.1095/biolreprod.109.081547

BIOLOGY OF REPRODUCTION **82,** 1151–1161 (2010)
Published online before print 17 February 2010.
DOI 10.1095/biolreprod.109.081547

Role of Ubiquitin C-Terminal Hydrolase-L1 in Antipolyspermy Defense of Mammalian Oocytes[1]

Andrej Susor,[2,3] Lucie Liskova,[3] Tereza Toralova,[3] Antonin Pavlok,[3] Katerina Pivonkova,[3] Pavla Karabinova,[3] Miloslava Lopatarova,[5] Peter Sutovsky,[4] and Michal Kubelka[3]

Institute of Animal Physiology and Genetics,[3] Academy of Sciences of the Czech Republic, Libechov, Czech Republic
Division of Animal Sciences,[4] Department of Obstetrics, Gynecology and Women's Health, University of Missouri-Columbia, Columbia, Missouri
University of Veterinary and Pharmaceutical Sciences,[5] Brno, Czech Republic

ABSTRACT

The ubiquitin-proteasome system regulates many cellular processes through rapid proteasomal degradation of ubiquitin-tagged proteins. Ubiquitin C-terminal hydrolase-L1 (UCHL1) is one of the most abundant proteins in mammalian oocytes. It has weak hydrolytic activity as a monomer and acts as a ubiquitin ligase in its dimeric or oligomeric form. Recently published data show that insufficiency in UCHL1 activity coincides with polyspermic fertilization; however, the mechanism by which UCHL1 contributes to this process remains unclear. Using UCHL1-specific inhibitors, we induced a high rate of polyspermy in bovine zygotes after in vitro fertilization. We also detected decreased levels in the monomeric ubiquitin and polyubiquitin pool. The presence of UCHL1 inhibitors in maturation medium enhanced formation of presumptive UCHL1 oligomers and subsequently increased abundance of K63-linked polyubiquitin chains in oocytes. We analyzed the dynamics of cortical granules (CGs) in UCHL1-inhibited oocytes; both migration of CGs toward the cortex during oocyte maturation and fertilization-induced extrusion of CGs were impaired. These alterations in CG dynamics coincided with high polyspermy incidence in in vitro-produced UCHL1-inhibited zygotes. These data indicate that antipolyspermy defense in bovine oocytes may rely on UCHL1-controlled functioning of CGs.

cortical granule, deubiquitinating, fertilization, in vitro fertilization, meiosis, oocyte, oocyte development, ovum, polyspermy, proteasome, ubiquitin, zygote

INTRODUCTION

The ubiquitin-proteasome system regulates many cellular processes via substrate-specific protein degradation [1–3] and protein stabilization [4]. Covalent conjugation of ubiquitin to its substrate proteins plays a crucial role in a wide variety of biological processes [5]. Posttranslational modification by ubiquitination can be reversed by deubiquitination, a mechanism that plays an important widely recognized role in regulation of ubiquitin-dependent pathways. The deubiquitinating enzymes (DUBs) have been implicated, for example, in cell growth, differentiation, oncogenesis, and development and in regulation of chromosome structure [6]. One such DUB, ubiquitin C-terminal hydrolase-L1 (UCHL1), is highly abundant in mammalian oocytes [7]. It is also expressed in neurons and in the testis [8, 9]; however, abnormal expression of UCHL1 is also found in many primary lung tumors [10, 11] and in colorectal cancer [12].

UCHL1 has relatively weak hydrolytic activity and catalyzes hydrolysis of C-terminal ubiquityl esters and amides in vitro; peptide-ubiquityl amides are preferred substrates of UCHL1 [13, 14]. This activity is thought to be critical for cytoplasmic protein degradation and for recycling free ubiquitin by cleaving ubiquitylated peptides that are products of proteasomal degradation of polyubiquitylated proteins [13, 14]. UCHL1 has also been shown to have ligase activity, which correlates with dimerization or oligomerization of the enzyme [15]. Crystallography findings support the idea that UCHL1 is a tightly regulated enzyme and suggest an enzymatic activation mediated by substrate binding [16]. UCHL1 in COS-7 cells is posttranslationally modified by monoubiquitin at lysine 157 (K157) near the active site [17]. Farnesylation of the C-terminus of membrane-associated UCHL1 has been demonstrated in neural cells [18], which may be important to UCHL1 association with organelle membranes and with the inner face of the plasma membrane in oocytes. It has been also suggested that UCHL1 plays an important role in apoptosis; UCHL1 directly interacts with and stabilizes the proapoptotic tumor suppressor protein TP53 through ubiquitination [19]. Accordingly, the lack of functional UCHL1 in the *gad* mutant mouse [20] results in the absence of a physiological apoptotic wave in the testis that is important for male fertility [21–23].

Of particular interest for the present study is the proposed role of UCHL1 in the prevention of abnormal polyspermic fertilization in mammals. Fertilization in mammals is characterized by formation of one male and one female pronucleus after incorporation of a single spermatozoon into an oocyte. Such a constellation of paternal and maternal chromatin leads to normal embryo development. However, fertilization by more than one spermatozoon, called polyspermy, causes aberrant

[1]Major funding was provided by grant GACR 524/07/1087. P.K. and T.T. were supported by grant 204/09/H084; L.L. was supported by grant GACR 524/09/P435. This work was supported in part by National Research Initiative Competitive grant 2007-01319 from the USDA Cooperative State Research, Education and Extension Service to P.S. and by seed funding from the Food for the 21st Century Program of the University of Missouri-Columbia to P.S. This study was also supported by grant MSM 6215712403 and by Institutional Research Concept IAPG AV0Z50450515.
[2]Correspondence: Andrej Susor, Institute of Animal Physiology and Genetics, Academy of Sciences of the Czech Republic, 277 21 Libechov, Czech Republic. FAX: 420 315 639 510;
e-mail: susor@iapg.cas.cz

Received: 22 September 2009.
First decision: 12 October 2009.
Accepted: 27 January 2010.

eISSN: 1529-7268 http://www.biolreprod.org
ISSN: 0006-3363

development and death of the embryo at an early stage of development [24, 25]. Active blocking of polyspermic fertilization is necessary to prevent incorporation of multiple spermatozoa into an oocyte. Mammalian oocytes utilize both extracellular zona pellucida (ZP)-mediated and plasma membrane-mediated blocking of polyspermy. Although little is known about plasma membrane blocking in mammals, fertilization results in ZP glycoprotein modifications caused by enzymes released after cortical granule (CG) extrusion [26]. Increased polyspermy incidence was reported during in vitro fertilization (IVF) of *gad* mutant mouse oocytes lacking functional UCHL1 [27] and in porcine zygotes treated with ubiquitin aldehyde (a specific inhibitor of UCHs) [28]; nevertheless, the mechanism by which UCHL1 and other related UCHs regulate polyspermy defense remains unclear.

MATERIALS AND METHODS

Oocyte Collection and Maturation In Vitro

Ovaries were obtained from a local slaughterhouse and transported to the laboratory in physiological saline at 20°C. They were briefly washed in 70% ethanol and then in physiological saline. Oocytes were obtained by aspiration of large antral follicles (>4 mm). Only oocytes surrounded by compact cumuli (cumulus-oocyte complexes [COCs]) were used for culture. The COCs were cultured in maturation medium [29] supplemented with 15% estrus cow serum (ECS) and 5 IU/ml of Suigonan PG-600 (Intervet International B.V.) at 38.5°C in an atmosphere of 5% CO_2 [29]. Samples were collected at 0 h (germinal vesicle stage [GV]), 24 h (metaphase II [MII]), and 20 h (1-cell zygote) after fertilization. At the end of culture, the cumulus cells were removed from oocytes by vortexing. Denuded oocytes were washed in PBS and stored at −80°C for immunoblotting experiments. Some oocytes and zygotes were evaluated for meiotic progression and fertilization by staining with 0.1 μg/ml of Hoechst 33258 (Sigma) and observed under an Olympus IX70 epifluorescence microscope.

Inhibition of UCHL1 in the Oocyte

To investigate the role of UCHL1 in the oocyte, the following specific inhibitors of UCHL1 were added to the medium at 20 μM concentration (unless stated otherwise) at the beginning of culture: C30 [30] (alternative designation LDN-57444 [662086; Merck]) and C16 [31] (kindly provided by Dr. Gregory D. Cuny, Harvard Center for Neurodegeneration and Repair, Brigham & Women's Hospital and Harvard Medical School, Boston, MA). C30 is a reversible, competitive, active site-directed isatin oxime with consistent preference for UCHL1 over UCHL3 by 28-fold. C16 is an uncompetitive inhibitor of UCHL1 that binds only to the Michaelis complex and not to free enzyme. Stock solutions of C16 and C30 were prepared in dimethyl sulfoxide (DMSO) (D2438; Sigma) and kept frozen at −20°C. Controls were treated with an equivalent amount of DMSO. Final working solutions of C16 and C30 were diluted immediately before usage. Meiotic progression was evaluated at 24 h after isolation (extrusion of first polar body [PB]). The COCs were washed thoroughly in fertilization medium (FM) before IVF.

In Vitro Fertilization

Frozen ejaculate from the same fertile bull (provided by the Czech Breeders Association), stored in sperm pellet form, was used in all experiments. Basic FM was used for sperm thawing, washing, and swim up [29]. Sperm pellets were plunged into 2 ml of FM warmed up to 39°C, centrifuged in conic tubes for 10 min at 250 × *g*, and washed twice in FM. After the second wash, sperm pellets were incubated for 10 min at 39°C and divided into two equal parts; each part was layered under 1 ml of FM in 8-ml tubes and then incubated for 10 min at 39°C for the swim-up procedure. The supernatants (2 × 0.7 ml) with motile spermatozoa were pooled and centrifuged. Spermatozoa were placed into each well of four-well Nunclon dishes (Thermo Fisher Scientific, Denmark) with 500 μl of FM supplemented with 1.5 mg/ml of crystallized bovine serum albumin (BSA), 0.25 mg/ml of D-penicillamin (Sigma), 2% fetal calf serum, and 5 IU/ml of heparin (Sigma). The final sperm concentration was 0.5×10^6 sperm per milliliter of FM. Washed COCs were coincubated with spermatozoa for 20 h at 38.5°C in an atmosphere of 5% CO_2. No inhibitors were added to FM during IVF. The number of pronuclei and CG status were assessed at 20 h after fertilization as already described.

Parthenogenetic Activation

Bovine oocyte maturation and in vitro embryo culture were performed as described previously [32]. C30 inhibitor was dissolved in DMSO and added to maturation medium at 20 μM concentration; DMSO alone was added to control maturation medium. After 24 h of maturation, oocytes were stripped of cumulus cells by vortexing. Oocytes were activated according to an established method [33] with slight modifications. Briefly, oocytes were incubated in 5 μM ionomycine (Sigma) in Tyrode lactate-Hepes supplemented with 3 mg/ml of BSA for 5 min and subsequently in 2 mM 6-DMAP (Sigma) in EmbryoAssist medium (Medicult) supplemented with 15% ECS for 5 h. After activation, oocytes were transferred into pure EmbryoAssist medium with ECS. Embryo development was examined at 32, 44, 56, 92, 120, 156, and 180 h after activation, and the numbers of 2-cell, 4-cell, early 8-cell, and late 8-cell embryos and morulae and blastocysts were counted at each time point.

In Vitro mRNA Production for Microinjection

The pCMVFL3 vector with cDNA clone (OVR010079H10) containing the full-length porcine *UCHL1* sequence (GenBank accession number AK234541.1) was a gift from Professor Hirohide Uenishi (National Institute of Agrobiological Sciences, Tsukuba, Japan). The porcine-specific protein sequence (Q6SEG5) was aligned to the bovine protein sequence (ENSBTAT00000006692) using BLAST analysis, and identity between both sequences was 96%. To generate the template for transcription, full-length porcine cDNA of *UCHL1* was cloned into the *Spe*I site (for N-terminal green fluorescent protein [GFP] tags) of the phageRNA (pRNA)-enhanced GFP (EGFP) or pRNA-empty vector containing a T3 promoter and *Xenopus* globin 5′ untranslated region (UTR), 3′ UTR, and Kozak sequences for high mRNA stability and efficient translation initiation [34]. *EGFP-UCHL1* mRNA and wild-type *UCHL1* mRNA for microinjection were produced by in vitro transcription of the linearized vector using mMESSAGE mMACHINE T3 kit (1348; Ambion). After in vitro transcription, mRNAs were immediately polyadenylated using Poly(A) Tailing kit (AM1350; Ambion) for stabilization. They were purified using RNeasy Mini kit (74104; Qiagen). Identity of products was confirmed by sequencing. *EGFP* mRNA for control microinjection was transcribed from an empty pRNA-EGFP vector. The mRNAs were aliquoted (5 μl) at 500 ng of RNA per microliter and stored at −80°C until used for microinjection.

Oocyte Microinjection

Freshly isolated GV-stage oocytes were partly denuded from cumulus cells and cultured for 1 h in manipulation medium (MM) without hormones. Oocytes were microinjected with 5 pl of the mRNA solution using an MIS-5000 micromanipulator (Burleigh; Exfo Life Sciences) and a PM 2000B4 microinjector (MicroData Instrument). Pipettes for microinjection were prepared using a P97 Pipette Puller (Sutter Instrument Company). The microinjection medium was the MM (110 mM NaCl, 10 mM glucose, 8 mM Hepes, 5 mM KCl, 2 mM $CaCl_2.H_2O$, 0.5 mM KH_2PO_4, 0.4 mM $MgSO_4.7H_2O$, 0.1% $NaHCO_3$, 1 mg/ml of polyvinyl alcohol, 0.2 mg/ml of sodium pyruvate, and antibiotics). Oocytes were microinjected with *Uchl1* mRNA with dextran-fluorescein isothiocyanate (FITC) or with *EGFP-UCHL1* mRNA. Control oocytes were injected with dextran-FITC (1 mg/ml, 70 kDa; Sigma) (Supplemental Fig. S1 available at www.biolreprod.org). Following microinjection, oocytes were incubated in MM with PG-600. Only oocytes displaying EGFP fluorescence or dextran-FITC fluorescence were used for analysis. Oocytes were dry frozen at −80°C for immunoblotting or fixed in 4% paraformaldehyde (16005; Sigma) for immunofluorescence, in which case they were mounted in an antifade medium containing DNA stain 4′,6′-diamidino-2-phenylindole (DAPI) and analyzed by confocal microscopy.

Immunoblotting of Oocyte Extracts

Unless stated otherwise, all reagents were obtained from Sigma. Exact numbers of oocytes (20, 50, or 100 oocytes per extract) were lysed in 3× Blue Loading Buffer (7722; Cell Signaling) with or without dithiothreitol (DTT) and then subjected to SDS-PAGE gel (12% or 15% acrylamide, 0.75-mm thick). To limit the amount of disulfide-bonded oligomers formed in cells, the thiol-blocking agent *N*-ethylmaleimide (NEM) was added to the cell lysis buffer [35, 36]. Proteins were transferred to Immobilon P membrane (Millipore Corporation) using a semidry blotting system (Whatman Biometra GmbH) for 30 min at 5 mA/cm^2. Blocking of the membrane was performed in 5% nonfat milk in Tris-buffered saline (TBS)-Tween buffer (TBS-T) (20 mM Tris, pH 7.4, 137 mM NaCl, and 0.5% Tween 20) for 1 h. After three washes for 10 min in TBS-T, the membrane was incubated overnight with the first antibody.

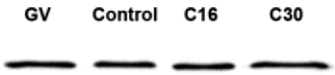

FIG. 1. The level of the monomeric form of UCHL1 does not change during oocyte maturation. Bovine oocytes were analyzed by immunoblotting (50 oocytes per lane). Protein lysates were prepared from GV-stage and MII-stage oocytes. Individual groups of MII oocytes were treated with UCHL1 inhibitor C16 or C30 or DMSO (vehicle solvent for inhibitors). A representative image from three independent experiments is shown.

All antibodies were diluted in 5% skim milk-TBS-T at 1:1000 dilution. UCHL1 was detected by mouse monoclonal antibody (58593; Santa Cruz Biochemicals) or by goat polyclonal antibody (5937; Chemicon). Antiubiquitin antibodies included mouse monoclonal antimonoubiquitin (0508; Sigma), mouse antipolyubiquitin (K^{63} linkage specific, PW0600; Biomol), and mouse antipolyubiquitin (58595; Santa Cruz Biochemicals). Washed membranes were incubated with appropriate horseradish peroxidase-conjugated secondary anti-IgG antibodies (1:10 000 dilution; Jackson Immunoresearch) in 5% nonfat milk-TBS-T for 1 h at room temperature. Protein bands were visualized by an ECL-PLUS detection system (GE Healthcare) according to the manufacturer's instructions. All Western blot experiments described in *Results* were performed at least two times, and representative images are shown in the figures. Band intensities were measured using ImageJ software (National Institutes of Health). Data were normalized to the number of oocytes (equal number of oocytes per line in each sample). The control was considered 100%.

Immunocytochemistry

For immunofluorescence microscopy, denuded and ZP-free oocytes (dezoned in 0.25% pronase) were washed in PBS, fixed for 60 min at 4°C in 4% paraformaldehyde in PBS, and again washed in PBS. Oocytes were permeabilized with 1% Triton X-100 for 20 min, washed and blocked for 2 h in 2% BSA in PBS, and incubated with primary antibody overnight at 4°C. All primary and secondary antibodies were diluted in 0.2% BSA in PBS. Anti-UCHL1 antibody (5937; Chemicon) was used at 1:500 dilution; antiubiquitin antibodies were used as already described. Oocytes were incubated with appropriate secondary antibodies (Alexa Fluor 488 and 543; Invitrogen) for 60 min at room temperature. As a control, oocytes were incubated with secondary antibody only. *Lens culinaris* agglutinin (LCA rhodamine, 1042; Vector Laboratories) was used as a marker of CGs [37]. F-actin was stained with 1 mg/ml of Phalloidin-Alexa Fluor 568 (12380; Molecular Probes). Oocytes and zygotes were mounted in mounting medium with DAPI (Vectashield; Vector Laboratories). To prevent deformities, 100-μm coverslip spacers (Zweckform) were used. Samples were examined under a Leica SP2 inverted confocal microscope equipped with an Acousto-Optical Beam Splitter (Leica Microsystems). Fluorescence intensities were measured using ImageJ software.

Statistical Analysis

Data were analyzed using SigmaStat 3.0 software (Jandel Scientific). *z*-Test was used for analysis of differences in proportions of characteristics of interest within groups. Student *t*-test or Mann-Whitney rank sum test was used for analysis of densitometric measurements. $P < 0.05$ was considered significant.

RESULTS

Protein Levels of UCHL1 Are Stable During Oocyte Maturation

An immunoblotting approach was used to detect expression of UCHL1 in bovine oocytes; the specific band of approximately 27 kDa (monomer form) was recognized and did not significantly change during oocyte maturation. We used two UCHL1-specific inhibitors, C16 and C30, to disrupt UCHL1 activity [30, 31]. Oocytes were treated with both inhibitors for 24 h at a concentration of 20 μM. We observed no difference in UCHL1 (27-kDa form) expression levels between GV- and MII-stage oocytes or any differences between control oocytes and oocytes treated with specific UCHL1 inhibitors ($P > 0.05$) (Fig. 1). Meiotic progression was not impaired in the presence of UCHL1 inhibitors (data not shown).

In summary, we observed stable levels of the monomeric form of UCHL1 during oocyte maturation. Inhibition of hydrolytic activity of UCHL1 did not block meiotic progression of bovine oocytes.

Subcellular Localization of UCHL1 in Bovine Oocytes

To study localization of UCHL1 in bovine oocytes, we used two different approaches. We microinjected oocytes with in vitro-synthesized *UCHL1* mRNA fused with EGFP (*EGFP-UCHL1*). This *UCHL1* mRNA was based on the porcine *UCHL1* sequence, which is highly homologous to the bovine sequence (98% amino acid sequence homology [see *Materials and Methods*]). Two different concentrations (125 or 250 ng/μl) of in vitro-synthesized mRNA were used. At 1 h after microinjection of 125 ng/μl of *EGFP-UCHL1* mRNA into GV-stage oocytes, the majority of EGFP signal was predominantly detected in cortical and subcortical regions (Fig. 2A). Low-level signal was visible throughout the cytoplasm and GV nucleoplasm (Fig. 2A). However, at the MII stage, EGFP-UCHL1 localized exclusively to the subcortical region (Fig. 2B). In contrast, oocytes injected with 250 ng/μl of *EGFP-UCHL1* mRNA were unable to progress beyond the MI stage of meiosis. EGFP-UCHL1 fluorescent signal in such mRNA-injected oocytes was detected in the oocyte cortex, subcortically, and in the perivitelline space (PVS). The differential interference contrast (DIC) images showed colocalization of this PVS signal with small droplets or vesicles (Fig. 2, E and F, arrows).

The specificity of localization of EGFP-UCHL1 was confirmed in control experiments using *EGFP* mRNA alone (125 or 250 ng/μl). EGFP signal was visible throughout the cytoplasm and was absent from the nucleus (Fig. 2, C and D).

These results were further confirmed by immunocytochemistry using specific anti-UCHL1 antibody (Fig. 3, A and B). Immunolocalization of UCHL1 agreed with EGFP-UCHL1 localization in microinjection experiments. The antibody labeled cortical and subcortical regions in GV-stage and MII-stage oocytes; in GV oocytes, fluorescent signal was also detected in the nucleus (Fig. 3A). Localization of native UCHL1 was unaffected in oocytes treated with C16 and C30 inhibitors (data not shown).

Inhibition of UCHL1 Causes Polyspermy During Bovine IVF

UCHL1 protein has been implicated in antipolyspermy defense in vitro in both mouse [27] and pig [28]. To explore the mechanistic basis for these observations, we studied the effects of downregulation of oocyte UCHL1 on bovine IVF. To investigate the role of UCHL1 during meiotic maturation of bovine oocytes, we treated oocytes with UCHL1-specific membrane-permeant inhibitors C16 and C30.

We did not use the RNA interference method, as UCHL1 expression is stable during oocyte maturation and its turnover is low (Supplemental Fig. S2). Because these inhibitors are highly specific [30, 31], we were able to use them at a relatively low concentration of 20 μM. Higher concentration of UCHL1-specific inhibitors (100 μM) did not block meiotic progression in bovine oocytes; however, 30% of MII-stage oocytes extruded all their chromosomes in the form of two PBs (Supplemental Fig. S3).

We then examined fertilization rates and occurrence of polyspermy after IVF in oocytes treated for the whole oocyte maturation period of 24 h with specific UCHL1 inhibitors (C16 and C30) and in control oocytes matured without inhibitors (with DMSO as a vehicle control). In the majority of zygotes

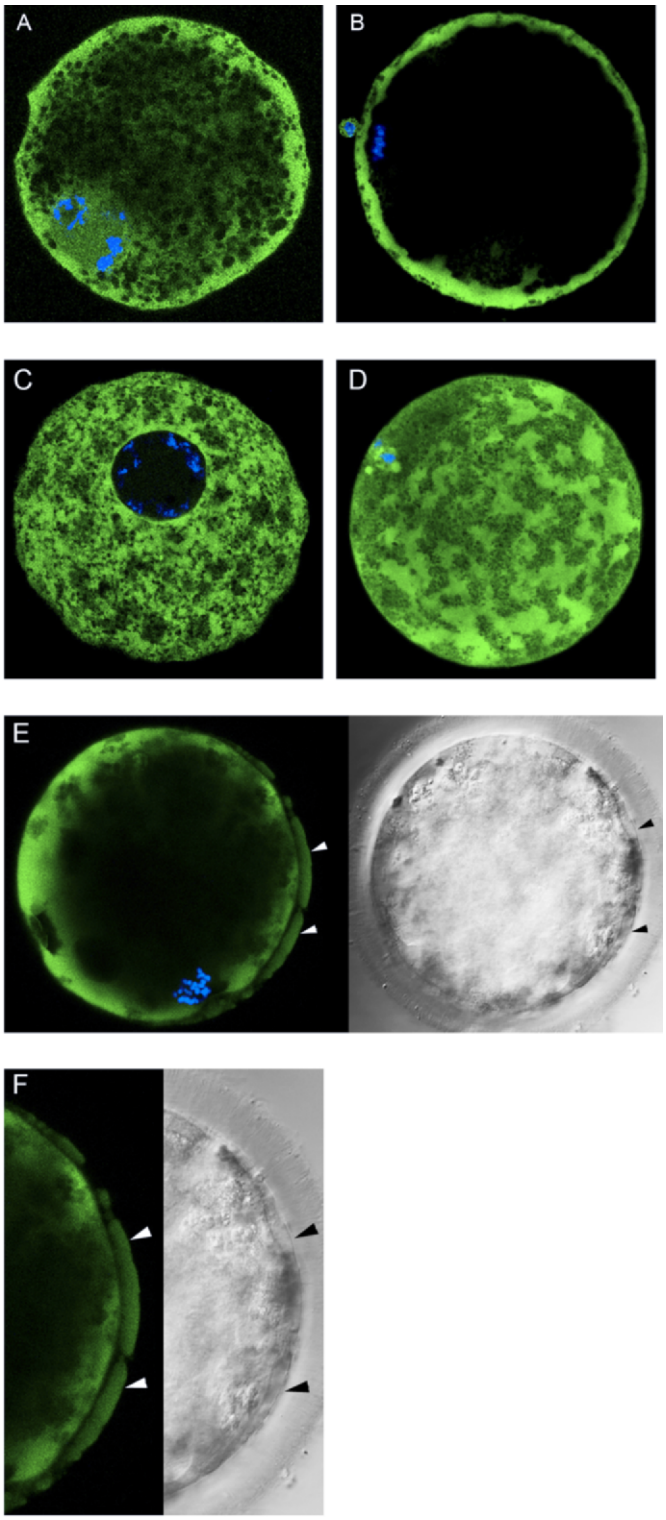

FIG. 2. Localization of GFP-tagged UCHL1 in bovine oocytes. **A**–**D**) Representative confocal images of bovine oocytes microinjected with 125 ng/μl of *UCHL1* mRNA. **A**) At 1 h after microinjection of mRNA, EGFP-UCHL1 protein is localized predominantly in the subcortical region, with low signal in the cytoplasm and some accumulation in the oocyte nucleus and GV (10 of 11 oocytes examined had the described phenotype). **B**) At 24 h after microinjection, oocytes reached MII, and EGFP-UCHL1 fluorescence was predominantly visible in the oocyte cortex (14 of 14 examined). **C**) As a negative control for EGFP-UCHL1, *EGFP* mRNA (125 ng/μl) was used, resulting in even distribution of EGFP throughout the ooplasm and complete exclusion from the nucleus at 1 h after microinjection (23 of 23 examined). **D**) Microinjected control oocytes with *EGFP* mRNA (125 ng/μl) at 24 h after microinjection (18 of 18 examined). **E**) Oocytes microinjected with 250 ng/μl of *EGFP-UCHL1* mRNA and arrested in MI; arrows indicate EGFP-UCHL1 fluorescence in the PVS. This fluorescence colocalizes with PVS membrane vesicles in the DIC image (10 of 10 examined). **F**) Detailed image of **E**. Green indicates EGFP-UCHL1 or EGFP; blue, DAPI used for DNA staining. Original magnification ×300 (**A**–**E**) and ×350 (**F**).

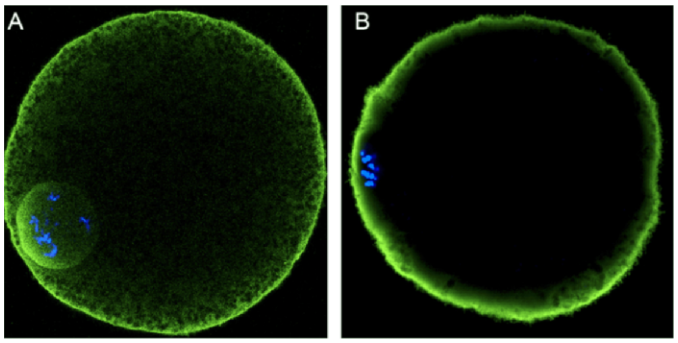

FIG. 3. Localization of native UCHL1. Polyclonal antibody against UCHL1 detects subcortical and nuclear accumulation of endogenous UCHL1 in a GV-stage oocyte (**A**) (22 of 22 examined) and an MII-stage oocyte (**B**) (19 of 19 examined). Green indicates UCHL1; blue, DAPI for DNA staining. Original magnification ×300.

that originated from oocytes treated with UCHL1 inhibitors, more than two pronuclei were found at 20 h after IVF (60% in the C16-treated group and 66% in the C30-treated group) (Fig. 4 and Table 1). When oocytes were stained for chromatin or DNA, the predominant pattern was the presence of three pronuclei in inhibitor-treated oocytes, suggestive of dispermic fertilization. In contrast, only 10% of dispermic or polyspermic zygotes were detected in vehicle control (DMSO [$P < 0.001$]), while the overall fertilization rate was not significantly different between treatments. These results suggest that, although inhibition of UCHL1 through meiosis does not impair nuclear maturation, the efficiency of antipolyspermy defense is reduced; thus, UCHL1 activity during in vitro maturation of bovine oocytes affects the rate of sperm penetration or incorporation during fertilization of MII oocytes.

Because developmental competence of embryos is impaired in polyspermy [38], we examined developmental competence of UCHL1 inhibitor-treated oocytes. We performed parthenogenic activation of oocytes treated with C30 (n = 59) and DMSO (n = 44). No significant difference was found in developmental competence of parthenotes produced from oocytes cultivated in 20 μM C30 compared with the control group ($P > 0.05$ for each developmental stage examined) (Fig. 5).

Failure of CG Translocation During Meiotic Maturation in UCHL1-Inhibited Oocytes

The foregoing results suggested that inhibition of UCHL1 aggravates polyspermy in vitro. We next sought to determine whether downregulation of UCHL1 function inhibits the landmark mechanism necessary for blocking polyspermy (i.e., CG maturation and CG extrusion or exocytosis). We focused on distribution changes of CGs in MII oocytes. In GV-stage oocytes, CGs form clusters; as oocytes progress through meiosis, CG clusters dissociate, and CGs invade the cortical region, forming a thin layer [37, 39]. We stained CGs with rhodamine-labeled LCA; for classification of CG distribution, we adopted the previously established terms of *oocyte-like*

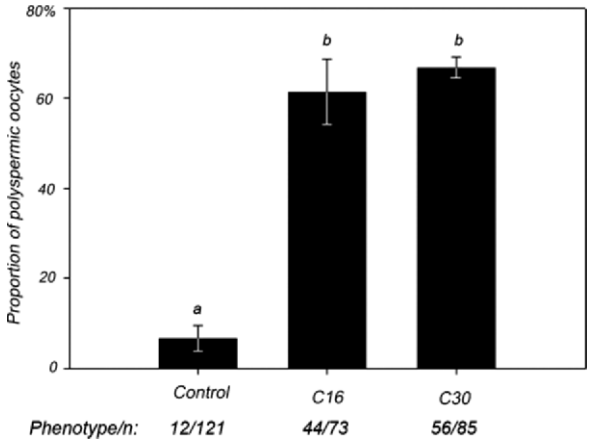

FIG. 4. Incidence of polyspermy in UCHL1 inhibitor-treated oocytes. Formation of supernumerary male pronuclei occurs in zygotes obtained by IVF of oocytes matured in the presence of UCHL1 inhibitor C16 or C30. Values from three independent replicates are shown. Different lowercase letters indicate statistical significance ($P < 0.001$).

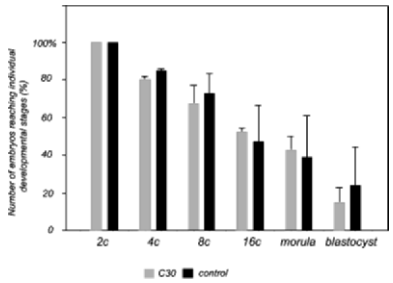

FIG. 5. Developmental competence of embryos after parthenogenetic activation. The numbers of embryos reaching individual developmental stages are shown on the y-axis. The number of 2-cell-stage (2c) embryos is considered 100%. The proportion of oocytes that do not develop beyond the 1-cell stage was not significantly different in C30-treated (38%) vs. control (34%) oocytes. Developmental competence was examined in two independent experiments; bars represent the mean ± SEM.

pattern (typical of GV stage), *intermediate* pattern, and *egg-like* pattern (typical of MII stage) [37].

Migration of CGs was indeed altered in oocytes treated with UCHL1 inhibitors C16 and C30 (Fig. 6, C and D). A majority of MII oocytes or eggs treated with inhibitors during in vitro maturation displayed an oocyte-like CG localization pattern similar to that of GV-stage oocytes (Fig. 6A). Karyokinesis or meiotic progression was not altered (data not shown). In control groups treated with DMSO, CGs relocalized uniformly to the cortical area of the oocyte, displaying an egg-like pattern at MII (Fig. 6B). Data on CG translocation are summarized in Figure 7 and Supplemental Table S1.

In GV-stage oocytes injected with 125 ng/μl of *EGFP-UCHL1* mRNA, redistribution of CGs was not impaired (Fig. 6E), At the 250 ng/μl concentration, *EGFP-UCHL1* mRNA blocked redistribution of CGs during oocyte maturation (Fig. 6F).

Inspired by these observations, we investigated if high polyspermy observed in inhibitor-treated zygotes coincided with impaired GC extrusion. Oocytes were matured in the presence of 20 μM C16 or C30, washed thoroughly, and fertilized using a standard IVF protocol without inhibitors. We observed high retention of CGs in inhibitor-matured zygotes (Fig. 8, B and C) but not in control zygotes at 20 h after fertilization (Fig. 8A). Data on CG extrusion are summarized in Figure 9 and Supplemental Table S2. Figure 10 shows the positive correlation between polyspermy ratio and CG extrusion at 20 h after IVF. Migration of CGs is a cytoskeleton-dependent process in which F-actin plays the major role [40, 41]. When we stained F-actin with Phalloidin-Alexa Fluor 568, we found greater abundance of transzonal projections (TZPs) in oocytes treated during in vitro maturation with C16 and C30 (Supplemental Fig. S4). The retraction or depolymerization of F-actin-rich TZPs is a hallmark of oocyte maturation, and their retention beyond the GV breakdown stage is indicative of cytoskeletal dysfunction.

Treatment of Oocytes with Specific UCHL1 Inhibitors Reduces Monoubiquitin Levels and Increases Protein Ubiquitination

UCHL1 maintains the cytoplasmic pool of unconjugated monoubiquitin by recycling polyubiquitin chains. Consequently, we monitored free monoubiquitin levels and polyubiquitin in oocytes treated with C30 and C16. The average free monoubiquitin level decreased by 50% to 70% compared with controls (Fig. 11B). Conversely, formation of polyubiquitin chains and ubiquitination of proteins were increased 4 to 5 times in MII-stage oocytes treated with inhibitors compared with GV-stage oocytes and DMSO-treated MII oocytes (Fig. 11A). Overexpression of UCHL1 in oocytes injected with 125 ng/μl of *EGFP-UCHL1* mRNA at the GV stage resulted in 2- to 4-fold increase of free ubiquitin (monoubiquitin) at 24 h after microinjection (Fig. 11C). In contrast, we detected no change in ubiquitination of proteins after microinjection (data not shown). Results were similar for both types of mRNA injected (*EGFP-UCHL1* and nontagged *UCHL1*) (Supplemental Fig. S1).

Taken together, these results demonstrate that UCHL1 promotes disassembly of polyubiquitin chains during meiotic maturation. Conversely, UCHL1 regulates formation of polyubiquitin chains in bovine oocytes.

Presumptive Oligomeric Forms of UCHL1 Increase in the Presence of UCHL1 Inhibitors

Increased formation of polyubiquitin chains and protein ubiquitination observed in the presence of UCHL1 inhibitors

TABLE 1. Polyspermy incidence in one-cell bovine zygotes 20 h post IVF.*

	Fertilization status			
Treatment	Normal fertilized (%)	Polyspermic (%)	Nonfertilized (%)	Total n
DMSO (control)	96 (79)[a]	12 (10)[a]	13 (11)[a]	121
C16 (20 μM)	14 (19)[b]	44 (60)[b]	15 (21)[a]	73
C30 (20 μM)	17 (20)[b]	56 (66)[b]	12 (14)[a]	85

* Number of pronuclei was counted in zygotes obtained by IVF of oocytes matured in the presence of UCHL1 inhibitors; data are from three independent experiments.
[a,b] Values with different superscript letters indicate statistical significance ($P < 0.001$).

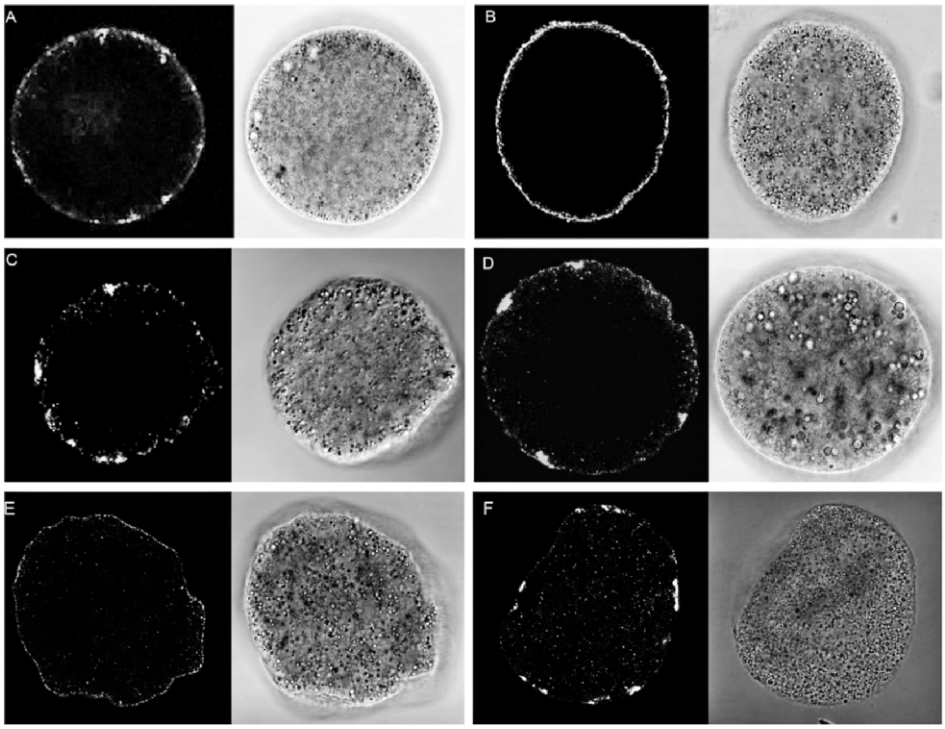

FIG. 6. Downregulation of UCHL1 affects migration or cortical translocation of CGs during oocyte maturation. **A–D**) Representative confocal images show GV-stage oocytes fixed immediately after isolation (**A**). **B**) Normal cortical migration of CGs (egg like) in an MII oocyte treated with DMSO. **C** and **D**) The CG distribution pattern in oocytes cultured in the presence of UCHL1 inhibitor C16 or C30 is similar to that of GV-stage (oocyte like) oocytes. **E** and **F**) Egg-like CG status in oocytes microinjected with 125 ng/μl of *EGFP-UCHL1* mRNA (**E**) and oocyte-like CG distribution following treatment with 250 ng/μl of *EGFP-UCHL1* mRNA concentration (**F**). Images are representative of three independent replicates. A summary of CG distribution for all groups is given in Supplemental Table S1. Original magnification ×175.

could account for increased ubiquitin ligase activity of dimeric and oligomeric forms of UCHL1 [15, 42]. By immunoblotting analysis, we identified several higher-mass UCHL1 bands at approximately 37 kDa (Supplemental Fig. S5) and in the range of 50–150 kDa (Fig. 12A). Expression of UCHL1 monomer did not change during meiotic maturation of bovine oocytes. Also, the 37-kDa UCHL1 band, presumably the monoubiquinated form of UCHL1 [17], did not change significantly during oocyte maturation (Supplemental Fig. S5). However, the content of presumptive UCHL1 oligomers (75–150 kDa) increased 6-fold in oocytes treated with C16 or C30 inhibitors (Fig. 12A).

Treatment of control and inhibitor-exposed oocyte lysates with 40 mM DTT (disulfide bond-reducing agent) and 4 mM NEM (alkylating reagent) was used to determine whether the presumptive UCHL1 oligomers could be linked by disulfide bonds. In the presence of DTT, both 50- and 75-kDa UCHL1 species were visible (Fig. 12A), likely corresponding to the presumptive dimer and oligomer of UCHL1, respectively. Without DTT, UCHL1 bands were observed at 50, 75, 100, and 150 kDa (Fig. 12B). These masses could correspond to multimerization of 27-kDa UCHL1, forming dimers, tetramers, and hexamers. The lack of presumptive oligomers within the range of 100–150 kDa in the presence of DTT strengthens the hypothesis that presumptive oligomers are cross-linked by disulfide bonds. In contrast, 50- and 75-kDa oligomers were not sensitive to DTT treatment. Finally, data shown in Figure 12 suggest increased formation of presumptive UCHL1 oligomers in the presence of inhibitors C16 and C30 during the in vitro maturation period.

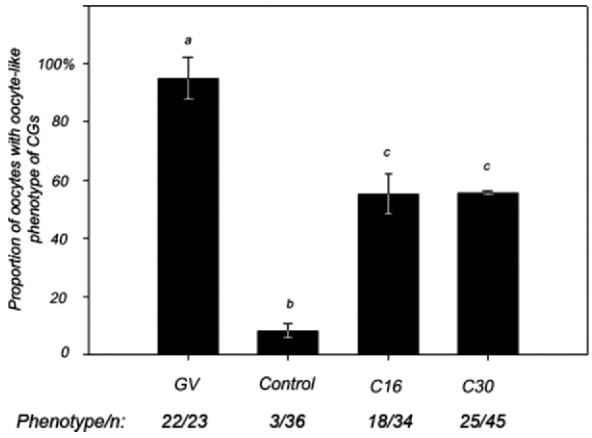

FIG. 7. Proportion of oocytes with the oocyte-like pattern of CG distribution in control and UCHL1 inhibitor-treated groups. Bars represent the mean ± SEM. Values from three independent experiments are given. Different lowercase letters indi cate statistical significance ($P < 0.001$).

Inhibition of UCHL1 Increases Formation of K63-Linked Multiubiquitin Chains

Polyubiquitin chains are linked through the C-terminal G76 residue of one ubiquitin molecule bound covalently to one of seven internal lysine residues (K6, K11, K27, K29, K33, K48, or K63) of another ubiquitin molecule [43–46]. In most cases, all molecules within an isopeptide polyubiquitin chain are linked at the same internal lysine position. Consequently, polyubiquitin chains can be distinguished based on the internal linkage site (e.g., K48 or K63 chains). In dimeric or oligomeric form, UCHL1 functions as a ubiquitin ligase that promotes formation of K63-linked polyubiquitin chains [15, 47]. To determine if this is the case in bovine oocytes, we performed immunocytochemical analysis of matured oocytes with mouse monoclonal antibody specific to K63-linked polyubiquitin chains. We found increased fluorescent signal in the cytoplasm for K63-linked ubiquitin antibody in oocytes treated with UCHL1 inhibitor C30 (Fig. 13B) compared with control oocytes treated with DMSO (Fig. 13A). Densitometric evaluation of these oocyte groups clearly showed higher fluorescence intensity (6.96 and 6.19, respectively) in C16- and C30-treated oocytes compared with 0.56 in the control group. These data support our hypothesis that inhibition of hydrolase

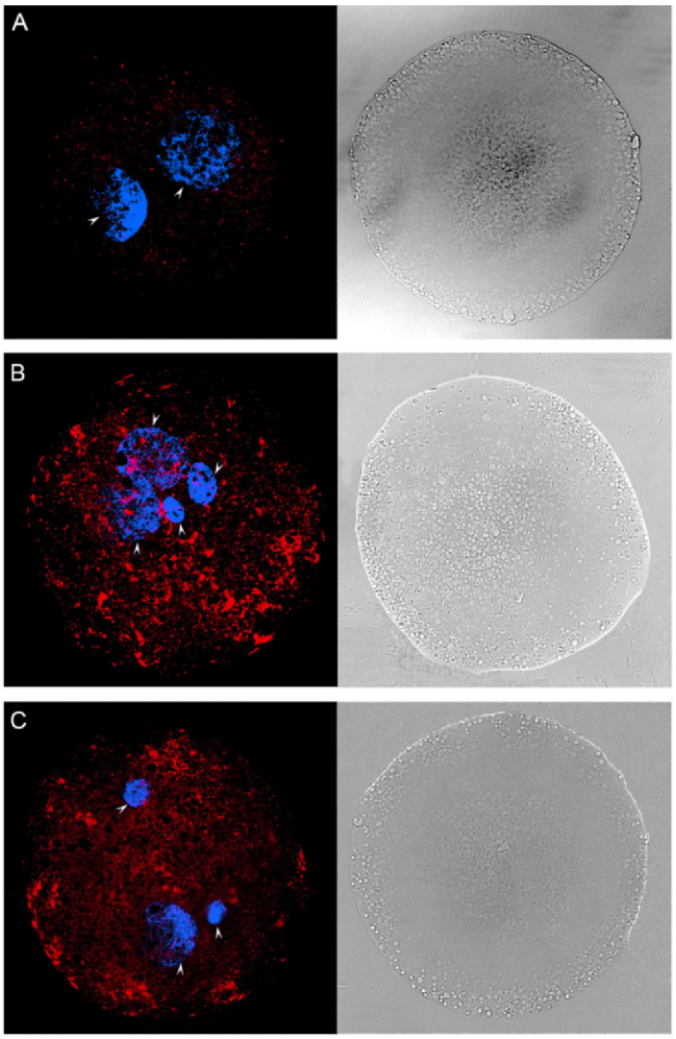

FIG. 8. Exocytosis of CGs in zygotes obtained by IVF of oocytes matured with UCHL1 inhibitor C16 or C30. Confocal images of zygotes at 20 h after IVF were acquired with identical settings for all treatments. **A**) Low fluorescence intensity of the LCA-rhodamine conjugate in a 1-cell zygote raised from oocytes matured in the presence of DMSO vehicle. **B** and **C**) Zygotes developed from oocytes matured with UCHL1 inhibitor C16 and C30, respectively. Images are representative of three independent experiments. The CG status in 1-cell zygotes for all groups is summarized in Supplemental Table S2. Original magnification ×230.

activity of UCHL1 stimulates ligase activity of this enzyme in bovine oocytes, resulting in increased protein stabilization or modification through K63-linked polyubiquitination.

DISCUSSION

UCHL1 is one of the most abundant proteins in mammalian oocytes [7, 48]. In the present study, we demonstrate that UCHL1 is involved in regulation of the fertilization process in bovine oocytes, most likely by controlling migration of CGs to the oocyte cortex during oocyte maturation. Such observations are consistent with the aforedescribed cortical and subcortical localization of UCHL1.

Treatment with specific inhibitors of UCHL1 activity leads to altered CG translocation during oocyte maturation and to increased polyspermy during bovine IVF. Our data show significant differences in polyspermy rates among oocytes in which UCHL1 was inhibited during in vitro maturation. Similar results were obtained using two inhibitors with

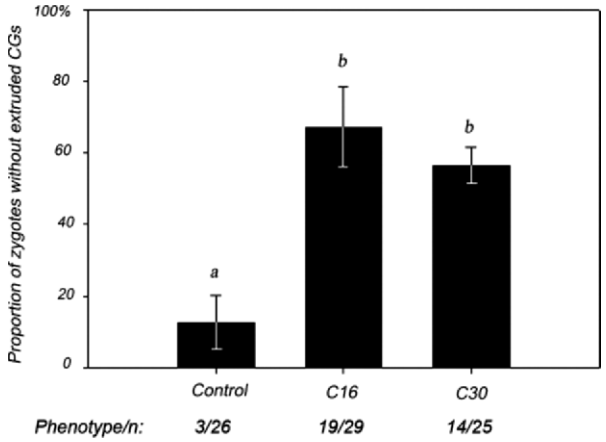

FIG. 9. Absence of CG exocytosis in 1-cell zygotes obtained by IVF of oocytes matured with UCHL1 inhibitor C16 or C30. Oocytes were vehicle treated (DMSO) or exposed to 20 μM C16 or C30 for 24 h. Bars represent the mean ± SEM. Values are from three independent experiments. Different lowercase letters indicate statistical significance ($P < 0.001$). The CG status in 1-cell zygotes for all groups is summarized in Supplemental Table S2.

different mechanisms of action, proving specific inhibition of UCHL1. Moreover, developmental competence was unaffected in parthenogenetic embryos that originated from inhibitor-treated oocytes. The higher rate of oocyte penetration by spermatozoa in such treated oocytes is in agreement with results from IVF of *gad* mice [27]. In *gad* mice, the modified *gad* allele encodes a truncated UCHL1 protein lacking a 42-amino acid segment containing a catalytic residue [13]. The *gad* mice have reduced fertility, with fewer pups per litter [27, 49]. High polyspermy was also reported by Yi et al. [28] in porcine oocytes fertilized in the presence of ubiquitin aldehyde, a specific nonpermeant inhibitor of UCH family enzymes.

Using immunocytochemical staining, we showed subcortical localization of native UCHL1 in bovine oocytes during maturation. Similar results were obtained when *EGFP-UCHL1* mRNA was expressed in oocytes. Cortical or subcortical localization of this protein was previously described in mouse and pig [27, 28]. In neural cells, two forms of UCHL1 are known, a soluble form and a membrane-anchored form, the

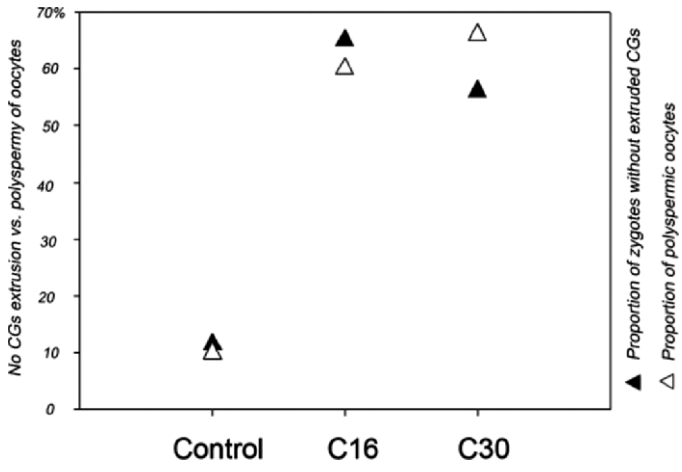

FIG. 10. Coincidence of polyspermy and failed CG extrusion in bovine zygotes treated with inhibitors of UCHL1. Analysis of data was obtained from experiments monitoring the number of oocyte-incorporated spermatozoa (see Fig. 4) and CG exocytosis at 20 h after IVF (see Fig. 8). Coefficient of determination $R^2 = 0.9275$.

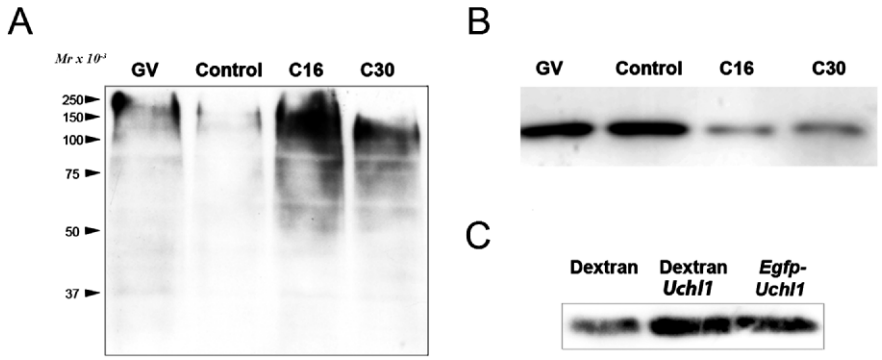

FIG. 11. Monoubiquitin and polyubiquitin levels in oocytes treated with UCHL1 inhibitors and after overexpression of UCHL1. UCHL1 was inhibited using 20 μM C16 or C30 during the in vitro maturation period (24 h). Control oocytes were cultured with inhibitor vehicle or solvent (DMSO) for the same period. **A**) In the presence of C16 or C30, chemiluminescence signal for ubiquitin is detected at a higher molecular mass in immunoblots; image is representative of two independent replicates. **B**) The monoubiquitin pool is decreased in C16- or C30-treated MII oocytes compared with control MII- and GV-stage oocytes; image is representative of three independent replicates. **C**) Microinjection of 125 ng/μl of *UCHL1* or *EGFP-UCHL1* mRNA increased the monoubiquitin pool in injected oocytes compared with control oocytes microinjected with dextran; image is representative of two indepenent replicates.

latter being farnesylated [18]. Farnesylation is a consensus signal for protein anchoring to a membrane. Previously, we reported three different isoforms of monomeric UCHL1 using two-dimensional gel electrophoresis [7]. These data suggest that oocytes carry posttranslationally modified UCHL1 forms that could coincide with differential localization of UCHL1 in the oocyte, including nuclear, subcortical, and membrane-bound forms. We detected fluorescent signal in the nucleus of GV-stage oocytes (Figs. 2A and 3A), which suggests that indigenous UCHL1 may also have an intranuclear function, as observed in somatic cells [50].

Differential localization of UCHL1 might regulate distinct pools of ubiquitin in an oocyte. Metaphase-anaphase transition during meiosis and mitosis depends on ubiquitination and proteasomal degradation of cyclin B, brought about by the ubiquitin ligase within the anaphase-promoting complex (APC) [51, 52]. Successful nuclear progression through meiosis in bovine oocytes treated with C16 and C30 inhibitors may be explained by the fact that the monoubiquitin pool, which is required for APC activity, is probably not completely depleted in the inhibitor-treated oocytes. Accordingly, meiotic progression is not impaired in the *gad* mouse [27]. Furthermore, other UCH family members present in the ooplasm (such as UCHL3) could compensate for the shortage of UCHL1 activity in both cases. Inhibition of UCHL1 in GV-stage pig oocytes seems to have a more dramatic effect compared with that in bovine oocytes; it leads to only a slight decrease in free ubiquitin but causes an early meiotic arrest at the MI stage [7]. Greater sensitivity of porcine oocytes to inhibition of UCHL1 could explain this observation.

Our experiments clearly show that UCHL1 is the mediator of monoubiquitin regeneration in oocytes. Overexpression of UCHL1 by mRNA microinjection significantly increased the ooplasmic monoubiquitin pool (Fig. 11C); however, no changes in polyubiquitination of proteins were seen in injected oocytes, as was also the case in inhibitor-treated oocytes (data not shown). Although the lower concentration of exogenous *UCHL1* mRNA did not have an effect on meiosis, 2-fold overexpression of UCHL1 impaired nuclear and cytoplasmic oocyte maturation. Impaired redistribution of CGs in these oocytes clearly shows that high expression of UCHL1 led oocytes to meiotic incompetence. Nuclear and cytoplasmic maturation are interconnected events [53]. Furthermore, a 2-fold increase in the concentration of microinjected mRNA led to inhibition of meiosis at the MI stage and coincided with the presence of UCHL1-containing vesicles in the PVS (Fig. 2, E and F). This might suggest that massive overexpression of

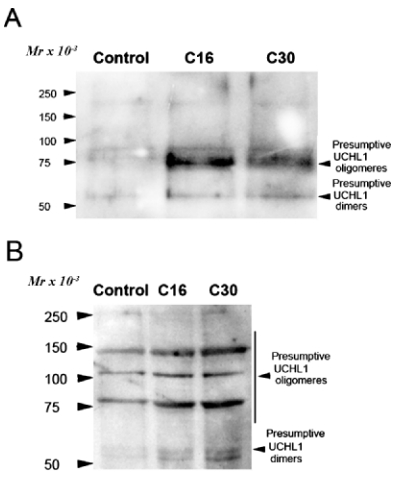

FIG. 12. Formation of presumptive UCHL1 oligomers in the presence of UCHL1 inhibitor C16 or C30. **A**) UCHL1 oligomers migrate predominantly at the 75-kDa level in the presence of the disulfide bond-reducing agent DTT. **B**) UCHL1 oligomers migrate at higher molecular mass when DTT is omitted from the oocyte lysis buffer. Images representative of two independent experiments are shown.

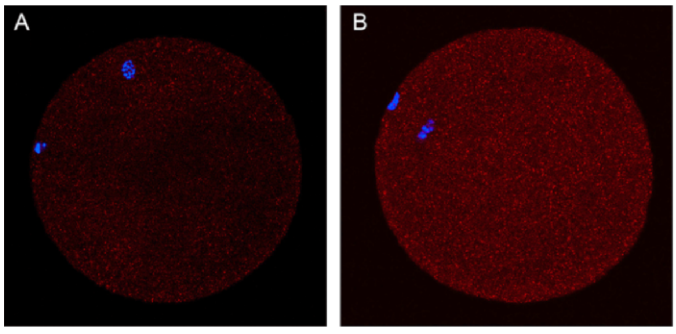

FIG. 13. Inhibition of UCHL1 stimulates formation of K63-linked polyubiquitin chains. **A**) Oocytes treated with DMSO only (0 of 10 examined). **B**) Immunocytochemical analysis shows higher fluorescence intensity of K63-linked ubiquitin chains in oocytes matured for 24 h in the presence of UCHL1 inhibitor (9 of 12 examined). Images were recorded with identical acquisition settings. Original magnification ×300.

UCHL1 can cause cell damage or even cell death, as reported in primary spermatocytes in transgenic mice overexpressing UCHL1 in testes [22] and in breast cancer cells [54]. Alternatively, UCHL1 could be responsible for stabilization of the oocyte plasma membrane.

Immunoblots showed increased formation of putative UCHL1 oligomers in oocytes treated with C16 or C30. Liu et al. [15] demonstrated that UCHL1 has two separate enzymatic functions; in the monomeric form, it has weak hydrolytic activity toward polyubiquitin chains, whereas in the oligomeric state it functions as a ubiquitin ligase that stabilizes proteins through K63-linked polyubiquitination [42]. This dual enzymatic function could explain regulation of ubiquitin levels in oocytes, whereby specific UCHL1 inhibitors reduce the monoubiquitin pool, leading to increased content of polyubiquitin chains and ubiquitinated proteins. Using immunocytochemistry, we demonstrated increased K63-linked polyubiquitination in UCHL1 inhibitor-treated oocytes, which is known to stabilize proteins [55]. Based on these results, we hypothesize that increased K63-linked polyubiquitination may lead to impaired reorganization of cortical cytoskeleton and consequently to altered migration of CGs.

Our data suggest that activity of the ubiquitin-proteasome pathway, altered by a reduced monoubiquitin pool and by increased ubiquitination of proteins in oocytes with downregulated UCHL1, was responsible for high polyspermy rates in bovine zygotes. Mechanisms controlling sperm-oocyte interactions during fertilization are ubiquitin-proteasome dependent [56–59]. Exocytosis of CGs in mammalian oocytes is required to produce ZP-associated blocking of polyspermy [26, 60], which is one of the most important factors affecting embryonic developmental competence [61]. It has been observed that CGs migrate to the periphery of the oocyte during maturation [37, 39]. The oocyte maturation-associated generation of CG asymmetry and the clustering of CGs in the oocyte cortex correlate with acquisition of exocytotic competence (i.e., the ability of CGs to undergo exocytosis in response to increased intracellular calcium concentration induced by the fertilizing spermatozoon) [62]. Inhibition of UCHL1 impairs cytoplasmic maturation by altering migration of CGs, which occurs during oocyte progression through meiosis [37]. Migration of CGs relies on oocyte microfilament cytoskeleton [40, 41]. While CGs in control oocytes migrated to the cortex, CGs in oocytes treated with UCHL1 inhibitors remained in the position similar to that of GV-stage oocytes; thus, CG exocytosis was impaired in the inhibitor-treated oocytes (following IVF). We rarely observed CG exocytosis at 20 h after IVF in 1-cell zygotes that were treated with C16 or C30 during oocyte maturation, which further supports the proposed relationship between CG distribution and exocytosis. Therefore, high polyspermy rates in IVF zygotes originating from inhibitor-treated oocytes are likely due to insufficient polyspermy blocking.

Very little is known about the role that ubiquitin and proteasomes play in cytoskeletal dynamics. Most evidence is from somatic cells. Csizmadia et al. [63] reported that the proteasome inhibitor EPI (experimental proteasome inhibitor) induced reorganization and relocation of nonubiquinated actin microfilaments and microtubules. Ubiquitination of the Lys118 residue of actin imparts one or more conformations that may be involved in regulation of muscle contractile activity [64]. Porcine COCs treated with proteasomal inhibitor MG132 had substantially increased total G- and F-actin, and this treatment inhibited the microfilament-driven process of cumulus expansion [65]. Downregulation of UCHL1 in podocytes altered podocyte morphology and localization of the F-actin component α-actinin-4 [66]. Similarly, we showed that F-actin containing TZPs, normally disappearing early during oocyte maturation, was much more abundant in oocytes when UCHL1 was inhibited; this suggests that TZPs and their depolymerization may affect CG migration or at the very least are reflective of microfilament dynamics in the maturing oocyte cortex. It has also been reported that downregulation of UCHL1 induces changes in somatic cell morphology that might be driven by cytoskeletal dynamics [30]. The DUB CYK-3 (*Caenorhabditis elegans* UCH, an orthologue of mammalian USP32) has specificity for cleaving ubiquitin from linear fusion proteins. In CYK-3-deficient *C. elegans* zygotes, actin-dependent events are hindered [67]. Those zygotes fail to undergo first embryonic cleavage; however, they form an F-actin ring at the presumptive cleavage site. Notably, we observed extrusion of the entire oocyte DNA content in the form of two PBs in oocytes treated with 100 μM C30 for 24 h. Mtango et al. [68] observed anomalous second PB extrusion in mouse oocytes injected with the UCH inhibitor ubiquitin aldehyde. Azoury et al. [69] suggested that the PB extrusion phenotype is dependent on actin filaments, which is in agreement with our results showing that UCHL1 is involved in cytoskeleton-driven CG reorganization.

Our results suggest that impaired function of UCHL1 correlates with failure of CG migration to the oocyte cortex and thus leads to insufficient antipolyspermy defense. Therefore, polyspermy observed in bovine oocytes treated with UCHL1 inhibitors, or in those oocytes that overexpressed UCHL1, is likely due to insufficient ZP-mediated polyspermy blocking in response to the lack of CG exocytosis after IVF, which is presumably induced by enhanced ligase activity of UCHL1. It is unclear how the ubiquitin-proteasome pathway is involved in regulation of cytoskeletal dynamics, which controls redistribution of CGs. Further study of UCHL1 ubiquitination may provide clues to physiological functions of this enzyme in cytoskeleton and broaden our understanding of CG dynamics. Overall, the finding that UCHL1 indirectly regulates CG redistribution during meiotic maturation of mammalian oocytes leads us to hypothesize that abnormal distribution of CGs causes high polyspermy rates under in vitro conditions. Further analysis of how UCHL1 and the ubiquitin-proteasome pathway in general promote redistribution of CGs during meiosis will be fertile ground for future studies.

ACKNOWLEDGMENTS

The authors are indebted to Dr. Hana Kovarova for helpful comments about the manuscript; to Patricia Jandurova, Lenka Travnickova, and Stepan Hladky for technical assistance; and to Ms. Kathy Craighead for manuscript editing. C16 and C30 inhibitors for this study were kindly provided by Dr. Gregory D. Cuny, Harvard Center for Neurodegeneration and Repair, Brigham & Women's Hospital and Harvard Medical School, Boston, MA. The pCMVFL3 vector with cDNA clone was kindly provided by Professor Hirohide Uenishi, National Institute of Agrobiological Sciences, Tsukuba, Japan.

REFERENCES

1. Etlinger JD, Gu M, Li X, Weitman D, Rieder RF. Protease/inhibitor mechanisms involved in ATP-dependent proteolysis. Revis Biol Celular 1989; 20:197–216.
2. Muller S, Schwartz LM. Ubiquitin in homeostasis, development and disease. Bioessays 1995; 17:677–684.
3. Sutovsky P. Ubiquitin-dependent proteolysis in mammalian spermatogenesis, fertilization, and sperm quality control: killing three birds with one stone. Microsc Res Tech 2003; 61:88–102.
4. Kaiser P, Huang L. Global approaches to understanding ubiquitination. Genome Biol 2005; 6:e233.
5. Hershko A, Ciechanover A, Varshavsky A. Basic Medical Research Award: the ubiquitin system. Nat Med 2000; 6:1073–1081.

6. Chung CH, Baek SH. Deubiquitinating enzymes: their diversity and emerging roles. Biochem Biophys Res Commun 1999; 266:633–640.
7. Susor A, Ellederova Z, Jelinkova L, Halada P, Kavan D, Kubelka M, Kovarova H. Proteomic analysis of porcine oocytes during in vitro maturation reveals essential role for the ubiquitin C-terminal hydrolase-L1. Reproduction 2007; 134:559–568.
8. Gong B, Leznik E. The role of ubiquitin C-terminal hydrolase L1 in neurodegenerative disorders. Drug News Perspect 2007; 20:365–370.
9. Kwon J, Wang YL, Setsuie R, Sekiguchi S, Sakurai M, Sato Y, Lee WW, Ishii Y, Kyuwa S, Noda M, Wada K, Yoshikawa Y. Developmental regulation of ubiquitin C-terminal hydrolase isozyme expression during spermatogenesis in mice. Biol Reprod 2004; 71:515–521.
10. Hibi K, Liu Q, Beaudry GA, Madden SL, Westra WH, Wehage SL, Yang SC, Heitmiller RF, Bertelsen AH, Sidransky D, Jen J. Serial analysis of gene expression in non-small cell lung cancer. Cancer Res 1998; 58:5690–5694.
11. Sasaki H, Yukiue H, Moriyama S, Kobayashi Y, Nakashima Y, Kaji M, Fukai I, Kiriyama M, Yamakawa Y, Fujii Y. Expression of the protein gene product 9.5, PGP9.5, is correlated with T-status in non-small cell lung cancer. Jpn J Clin Oncol 2001; 31:532–535.
12. Yamazaki T, Hibi K, Takase T, Tezel E, Nakayama H, Kasai Y, Ito K, Akiyama S, Nagasaka T, Nakao A. PGP9.5 as a marker for invasive colorectal cancer. Clin Cancer Res 2002; 8:192–195.
13. Larsen CN, Price JS, Wilkinson KD. Substrate binding and catalysis by ubiquitin C-terminal hydrolases: identification of two active site residues. Biochemistry 1996; 35:6735–6744.
14. Larsen CN, Krantz BA, Wilkinson KD. Substrate specificity of deubiquitinating enzymes: ubiquitin C-terminal hydrolases. Biochemistry 1998; 37:3358–3368.
15. Liu Y, Fallon L, Lashuel HA, Liu Z, Lansbury PT Jr. The UCH-L1 gene encodes two opposing enzymatic activities that affect α-synuclein degradation and Parkinson's disease susceptibility. Cell 2002; 111:209–218.
16. Das C, Hoang QQ, Kreinbring CA, Luchansky SJ, Meray RK, Ray SS, Lansbury PT, Ringe D, Petsko GA. Structural basis for conformational plasticity of the Parkinson's disease-associated ubiquitin hydrolase UCHL1. Proc Natl Acad Sci U S A 2006; 103:4675–4680.
17. Meray RK, Lansbury PT Jr. Reversible monoubiquitination regulates the Parkinson disease-associated ubiquitin hydrolase UCH-L1. J Biol Chem 2007; 282:10567–10575.
18. Liu Z, Meray RK, Grammatopoulos TN, Fredenburg RA, Cookson MR, Liu Y, Logan T, Lansbury PT Jr. Membrane-associated farnesylated UCH-L1 promotes alpha-synuclein neurotoxicity and is a therapeutic target for Parkinson's disease. Proc Natl Acad Sci U S A 2009; 106:4635–4640.
19. Yu J, Tao Q, Cheung KF, Jin H, Poon FF, Wang X, Li H, Cheng YY, Röcken C, Ebert MP, Chan AT, Sung JJ. Epigenetic identification of ubiquitin carboxyl-terminal hydrolase L1 as a functional tumor suppressor and biomarker for hepatocellular carcinoma and other digestive tumors. Hepatology 2008; 48:508–518.
20. Saigoh K, Wang YL, Suh JG, Yamanishi T, Sakai Y, Kiyosawa H, Harada T, Ichihara N, Wakana S, Kikuchi T, Wada K. Intragenic deletion in the gene encoding ubiquitin carboxy-terminal hydrolase in gad mice. Nat Genet 1999; 23:47–51.
21. Kwon J, Mochida K, Wang YL, Sekiguchi S, Sankai T, Aoki S, Ogura A, Yoshikawa Y, Wada K. Ubiquitin C-terminal hydrolase L-1 is essential for the early apoptotic wave of germinal cells and for sperm quality control during spermatogenesis. Biol Reprod 2005; 73:29–35.
22. Wang YL, Liu W, Sun YJ, Kwon J, Setsuie R, Osaka H, Noda M, Aoki S, Yoshikawa Y, Wada K. Overexpression of ubiquitin carboxyl-terminal hydrolase L1 arrests spermatogenesis in transgenic mice. Mol Reprod Dev 2006; 73:40–49.
23. Kwon J, Wang YL, Setsuie R, Sekiguchi S, Sato Y, Sakurai M, Noda M, Aoki S, Yoshikawa Y, Wada K. Two closely related ubiquitin C-terminal hydrolase isozymes function as reciprocal modulators of germ cell apoptosis in cryptorchid testis. Am J Pathol 2004; 165:1367–1374.
24. Hunter RH. Sperm-egg interactions in the pig: monospermy, extensive polyspermy, and the formation of chromatin aggregates. J Anat 1976; 122:43–59.
25. Hunter RH. Oviduct function in pigs, with particular reference to the pathological condition of polyspermy. Mol Reprod Dev 1991; 29:385–391.
26. Ducibella T. The cortical reaction and development of activation competence in mammalian oocytes. Hum Reprod Update 1996; 2:29–42.
27. Sekiguchi S, Kwon J, Yoshida E, Hamasaki H, Ichinose S, Hideshima M, Kuraoka M, Takahashi A, Ishii Y, Kyuwa S, Wada K, Yoshikawa Y. Localization of ubiquitin C-terminal hydrolase L1 in mouse ova and its function in the plasma membrane to block polyspermy. Am J Pathol 2006; 169:1722–1729.
28. Yi YJ, Manandhar G, Sutovsky M, Li R, Jonáková V, Oko R, Park CS, Prather RS, Sutovsky P. Ubiquitin C-terminal hydrolase-activity is involved in sperm acrosomal function and anti-polyspermy defense during porcine fertilization. Biol Reprod 2007; 77:780–793.
29. Pavlok A, Lapathitis G, Cech S, Kubelka M, Lopatárová M, Holý L, Klíma J, Motlík J, Havlícek V. Simulation of intrafollicular conditions prevents GVBD in bovine oocytes: a better alternative to affect their developmental capacity after two-step culture. Mol Reprod Dev 2005; 71:197–208.
30. Liu Y, Lashuel HA, Choi S, Xing X, Case A, Ni J, Yeh LA, Cuny GD, Stein RL, Lansbury PT Jr. Discovery of inhibitors that elucidate the role of UCH-L1 activity in the H1299 lung cancer cell line. Chem Biol 2003; 10:837–846.
31. Mermerian AH, Case A, Stein RL, Cuny GD. Structure-activity relationship, kinetic mechanism, and selectivity for a new class of ubiquitin C-terminal hydrolase-L1 (UCH-L1) inhibitors. Bioorg Med Chem Lett 2007; 17:3729–3732.
32. Pavlok A, Lucas-Hahn A, Niemann H. Fertilization and developmental competence of bovine oocytes derived from different categories of antral follicles. Mol Reprod Dev 1992; 31:63–67.
33. Susko-Parrish JL, Leibfried-Rutledge ML, Northey DL, Schutzkus V, First NL. Inhibition of protein kinases after an induced calcium transient causes transition of bovine oocytes to embryonic cycles without meiotic completion. Dev Biol 1994; 166:729–739.
34. McGuinness BE, Anger M, Kouznetsova A, Gil-Bernabé AM, Helmhart W, Kudo NR, Wuensche A, Taylor S, Hoog C, Novak B, Nasmyth K. Regulation of APC/C activity in oocytes by a Bub1-dependent spindle assembly checkpoint. Curr Biol 2009; 19:369–380.
35. Carleton M, Brown DT. The formation of intramolecular disulfide bridges is required for induction of the Sindbis virus mutant ts23 phenotype. J Virol 1997; 71:7696–7703.
36. Opstelten DJ, Wallin M, Garoff H. Moloney murine leukemia virus envelope protein subunits, gp70 and Pr15E, form a stable disulfide linked complex. J Virol 1998; 72:6537–6545.
37. Connors A, Kanatsu-Shinohara M, Schultz RM, Kopf RS. Involvement of the cytoskeleton in the movement of cortical granules during oocyte maturation, and cortical granule anchoring in mouse eggs. Dev Biol 1998; 200:103–115.
38. Santos P, Chaveiro A, Simoes N, Moreira da Silva F. Bovine oocyte quality in relation to ultrastructural characteristics of zona pellucida, polyspermic penetration and developmental competence. Reprod Domest Anim 2008; 43:685–689.
39. Wang WH, Sun QY, Hosoe M, Shioya Y, Day BN. Quantified analysis of cortical granule distribution and exocytosis of porcine oocytes during meiotic maturation and activation. Biol Reprod 1997; 56:1376–1382.
40. Sun QY, Lai L, Park KW, Kühholzer B, Prather RS, Schatten H. Dynamic events are differently mediated by microfilaments, microtubules, and mitogen-activated protein kinase during porcine oocyte maturation and fertilization in vitro. Biol Reprod 2001; 64:879–889.
41. Sun QY, Schatten H. Regulation of dynamic events by microfilaments during oocyte maturation and fertilization. Reproduction 2006; 31:193–205.
42. Doss-Pepe EW, Chen L, Madura K. Alpha-synuclein and parkin contribute to the assembly of ubiquitin lysine 63-linked multiubiquitin chains. J Biol Chem 2005; 280:16619–16624.
43. Johnson ES, Ma PC, Ota IM, Varshavsky A. A proteolytic pathway that recognizes ubiquitin as a degradation signal. J Biol Chem 1995; 270:17442–17456.
44. Hershko A, Ciechanover A. The ubiquitin system. Annu Rev Biochem 1998; 67:425–479.
45. Peng J, Schwartz D, Elias JE, Thoreen CC, Cheng D, Marsischky G, Roelofs J, Finley D, Gygi SP. A proteomics approach to understanding protein ubiquitination. Nat Biotechnol 2003; 21:921–926.
46. Kim HT, Kim KP, Lledias F, Kisselev AF, Scaglione KM, Skowyra D, Gygi SP, Goldberg AL. Certain pairs of ubiquitin-conjugating enzymes (E2s) and ubiquitin-protein ligases (E3s) synthesize nondegradable forked ubiquitin chains containing all possible isopeptide linkages. J Biol Chem 2007; 282:17375–17386.
47. Setsuie R, Wada K. The functions of UCH-L1 and its relation to neurodegenerative diseases. Neurochem Int 2007; 51:105–111.
48. Massicotte L, Coenen K, Mourot M, Sirard MA. Maternal housekeeping proteins translated during bovine oocyte maturation and early embryo development. Proteomics 2006; 6:3811–3820.
49. Yamazaki K, Wakasugi N, Sakakibara A, Tomita T. Reduced fertility in gracile axonal dystrophy (gad) mice. Jikken Dobutsu 1988; 37:195–199.

50. Caballero OL, Resto V, Patturajan M, Meerzaman D, Guo MZ, Engles J, Yochem R, Ratovitski E, Sidransky D, Jen J. Interaction and colocalization of PGP9.5 with JAB1 and p27(Kip1). Oncogene 2002; 21:3003–3010.
51. Hershko A. Mechanisms and regulation of the degradation of cyclin B. Philos Trans R Soc Lond B Biol Sci 1999; 354:1571–1576.
52. Morgan DO. Regulation of the APC and the exit from mitosis. Nat Cell Biol 1999; 2:47–53.
53. Ferreira EM, Vireque AA, Adona PR, Meirelles FV, Ferriani RA, Navarro PA. Cytoplasmic maturation of bovine oocytes: structural and biochemical modifications and acquisition of developmental competence. Theriogenology 2009; 71:836–848.
54. Wang WJ, Li QQ, Xu JD, Cao XX, Li HX, Tang F, Chen Q, Yang JM, Xu ZD, Liu XP. Over-expression of ubiquitin carboxy terminal hydrolase-L1 induces apoptosis in breast cancer cells. Int J Oncol 2008; 33:1037–1045.
55. Hofmann RM, Pickart CM. In vitro assembly and recognition of Lys-63 polyubiquitin chains. J Biol Chem 2001; 276:27936–27943.
56. Sakai N, Sawada MT, Sawada H. Non-traditional roles of ubiquitin-proteasome system in fertilization and gametogenesis. Int J Biochem Cell Biol 2004; 36:776–784.
57. Sun QY, Fuchimoto D, Nagai T. Regulatory roles of ubiquitin-proteasome pathway in pig oocyte meiotic maturation and fertilization. Theriogenology 2004; 62:245–255.
58. Sutovsky P, Manandhar G, McCauley TC, Caamaño JN, Sutovsky M, Thompson WE, Day BN. Proteasomal interference prevents zona pellucida penetration and fertilization in mammals. Biol Reprod 2004; 71:1625–1637.
59. Yi YJ, Manandhar G, Oko RJ, Breed WG, Sutovsky P. Mechanism of sperm-zona pellucida penetration during mammalian fertilization: 26S proteasome as a candidate egg coat lysin. Soc Reprod Fertil Suppl 2007; 63:385–408.
60. Hoodbhoy T, Talbot P. Mammalian cortical granules: contents, fate, and function. Mol Reprod Dev 1994; 39:439–448.
61. Bembenek JN, Richie CT, Squirrell JM, Campbell JM, Eliceiri KW, Poteryaev D, Spang A, Golden A, White JG. Cortical granule exocytosis in C. elegans is regulated by cell cycle components including separase. Development 2007; 134:3837–3848.
62. Ducibella T, Kurasawa S, Duffy P, Kopf GS, Schultz RM. Regulation of the polyspermy block in the mouse egg: maturation-dependent differences in cortical granule exocytosis and zona pellucida modifications induced by inositol 1,4,5-trisphosphate and an activator of protein kinase C. Biol Reprod 1993; 48:1251–1257.
63. Csizmadia V, Raczynski A, Csizmadia E, Fedyk ER, Rottman J, Alden CL. Effect of an experimental proteasome inhibitor on the cytoskeleton, cytosolic protein turnover, and induction in the neuronal cells in vitro. Neurotoxicology 2008; 2:232–243.
64. Burgess S, Walker M, Knight PJ, Sparrow J, Schmitz S, Offer G, Bullard B, Leonard K, Holt J, Trinick J. Structural studies of arthrin: monoubiquitinated actin. J Mol Biol 2004; 341:1161–1173.
65. Yi YJ, Nagyova E, Manandhar G, Procházka R, Sutovsky M, Park CS, Sutovsky P. Proteolytic activity of the 26S proteasome is required for the meiotic resumption, germinal vesicle breakdown, and cumulus expansion of porcine cumulus-oocyte complexes matured in vitro. Biol Reprod 2008; 78:115–126.
66. Meyer-Schwesinger C, Meyer TN, Munster S, Klug P, Saleem M, Helmchen U, Stahl RAK. A new role for the neuronal ubiquitin C-terminal hydrolase-L1 (UCH-L1) in podocyte process formation and podocyte injury in human glomerulopathies. J Pathol 2009; 217:452–464.
67. Kaitna S, Schnabel H, Schnabel R, Hyman AA, Glotzer M. A ubiquitin C-terminal hydrolase is required to maintain osmotic balance and execute actin-dependent processes in the early C. elegans embryo. J Cell Sci 2002; 115:2293–2302.
68. Mtango NR, Sutovsky M, Zhong Z, Vandevoort K, Latham KE, Sutovsky P. Roles of de-ubiquitinating enzymes UCHL1 and UCHL3 in oocyte maturation, fertilization, and zygotic development. In: Abstracts of the 42nd Annual Meeting of the Society for the Study of Reproduction, July 18–22, 2009, Pittsburgh, Pennsylvania. Biol Reprod 2009; 81(Suppl): Abstract 329.
69. Azoury J, Verlhac MH, Dumont J. Actin filaments: key players in the control of asymmetric divisions in mouse oocytes. Biol Cell 2009; 10:69–76.